



ELSEVIER

Contents lists available at ScienceDirect

European Journal of Pharmacology

journal homepage: www.elsevier.com/locate/ejphar

Molecular and cellular pharmacology

Melatonin affects voltage-dependent calcium and potassium currents in MCF-7 cell line cultured either in growth or differentiation medium

Roberta Squecco^a, Alessia Tani^b, Sandra Zecchi-Orlandini^a,
Lucia Formigli^b, Fabio Francini^{a,*}

^a Department of Experimental and Clinical Medicine, Section of Physiological Sciences, University of Florence, 50134 Florence, Italy^b Department of Experimental and Clinical Medicine, Section of Anatomy and Histology, University of Florence, 50134 Florence, Italy

ARTICLE INFO

Article history:

Received 24 November 2014

Received in revised form

24 March 2015

Accepted 25 March 2015

Available online 3 April 2015

Keywords:

Melatonin

Voltage-dependent Ca²⁺ currentsVoltage-dependent K⁺ currents

Electrophysiology

Chemical compounds studied in this article:

α-Dendrotoxin (PubChem SID: 135651983)

Chromanol (PubChem CID: 92890)

Iberiotoxin (PubChem CID: 16132435)

Melatonin (PubChem CID: 896)

Nifedipine (PubChem CID: 4485)

ABSTRACT

Big efforts have been dedicated up to now to identify novel targets for cancer treatment. The peculiar biophysical profile and the atypical ionic channels activity shown by diverse types of human cancers suggest that ion channels may be possible targets in cancer therapy. Earlier studies have shown that melatonin exerts an oncostatic action on different tumors. In particular, it was shown that melatonin was able to inhibit growth/viability and proliferation, to reduce the invasiveness and metastatic properties of human estrogen-sensitive breast adenocarcinoma MCF-7 cell line cultured in growth medium, with substantial impairments of epidermal growth factor (EGF) and Notch-1-mediated signaling. The purpose of this work was to evaluate on MCF-7 cells the possible effects of melatonin on the biophysical features known to have a role in proliferation and differentiation, by using the patch-clamp technique. Our results show that in cells cultured in growth as well as in differentiation medium melatonin caused a hyperpolarization of resting membrane potential paralleled by significant changes of the inward Ca²⁺ currents (T- and L-type), outward delayed rectifier K⁺ currents and cell capacitance. All these effects are involved in MCF-7 growth and differentiation. These findings strongly suggest that melatonin, acting as a modulator of different voltage-dependent ion channels, might be considered a new promising tool for specifically disrupting cell viability and differentiation pathways in tumour cells with possible beneficial effects on cancer therapy.

© 2015 Elsevier B.V. All rights reserved.

1. Introduction

Conventional chemotherapy is not always successful and usually accompanied by systemic toxicity and detrimental side effects. Thus, growing attempts are made to identify novel targets for cancer therapy.

The diverse types of human cancers may show a peculiar biophysical profile with an atypical ion channels activity (Abdul et al., 2003; Arcangeli et al., 2009). In such perspective, it might be worth to better characterize this issue with the aim of designing efficient ionic channel inhibitors/modulators that may potentially affect cancer therapy. Functional relationship exists between resting

membrane potential, K⁺ channel type expression and cell functions such as proliferation and differentiation (Asher et al., 2010; Cos and Sánchez-Barceló, 2003; Enomoto et al., 1986; Wang, 2004). Resting membrane potential is typically more depolarized in undifferentiated respect to differentiated cells (O'Grady and Lee, 2005; Pardo, 2004) and in cancer cells respect to terminally differentiated cells (Kunzelmann, 2005). Of interest, resting membrane potential and the type and amount of K⁺ and Ca²⁺ currents change during both cell cycle and differentiation (Blackiston et al., 2009; Sundelacruz et al., 2009) and are atypically modified in cancer cells (Becchetti, 2011; Bielanska et al., 2009; Haren et al., 2010; Lang et al., 2003; Ohkubo and Yamazaki, 2012; Ouadid-Ahidouch and Ahidouch, 2008).

By multidisciplinary approach, it was demonstrated on MCF-7 cell line (Margheri et al., 2012) that growth/viability and proliferation is significantly reduced by the treatment with melatonin, the hormone mostly produced by the pineal gland (Jablonska et al., 2013).

Moreover, preclinical in vitro and in vivo studies and clinical trials showed that melatonin was able to exert an oncostatic action on different tumors (Girgert et al., 2009; Hill et al., 2009, 2011a,b; Jung and Ahmad, 2006; Sánchez-Barceló et al., 2012; Srinivasan et al., 2008), to increase the efficacy of chemotherapy when used

Abbreviations: α-DTX, α-dendrotoxin; Chr, chromanol; HP, holding potential; IbTx, iberiotoxin; I_{BK}, voltage- and Ca²⁺-dependent delayed-rectifier iberiotoxin-sensitive K⁺ current; IKCa, intermediate-conductance Ca²⁺-activated K⁺ channels; I_{Ca,L}, L-type Ca²⁺ current; I_{Ca,T}, T-type Ca²⁺ current; I_{Ks}, slowly activating chromanol-sensitive K⁺ current; I_{K(V)}, fast activating α-dendrotoxin-sensitive K⁺ current; MLT, melatonin; MT1, melatonin receptor 1; MTS, 3-(4,5-dimethylthiazol-2-yl)-5-(3-carboxymethoxyphenyl)-2-(4-sulfophenyl)-2Htetrazolium assay; RMP, resting membrane potential

* Corresponding author. Tel.: +39 055 2751629; fax: +39 055 2751640.

E-mail address: fabio.francini@unifi.it (F. Francini).<http://dx.doi.org/10.1016/j.ejphar.2015.03.068>

0014-2999/© 2015 Elsevier B.V. All rights reserved.

in adjuvant settings and to decrease the side effects (Vijayalaxmi et al., 2002). Since proliferation and differentiation are typical of any cell system and are carefully regulated in the course of physiological development and life cycle, tumor evolution must imply a deregulation of their morphofunctional features.

In the present study, we evaluated the electrophysiological properties and the effects of melatonin on MCF-7 cells cultured in either growth or differentiation medium focusing our attention on ion channels as possible novel targets involved in cancer pathophysiology. In particular, by electrophysiological technique, we evaluated the action of melatonin on resting membrane potential and on voltage-dependent ionic channels known to play a role in proliferation (Baglioni et al., 2012; Bertolesi et al., 2002; Currò, 2014; Enomoto et al., 1986; Gamper et al., 2002; Girgert et al., 2009; Grant et al., 2009; Gray et al., 2004; Haren et al., 2010; Kunzelmann, 2005).

The rationale for this research originates from the evidence that several ionic channels have a key role in proliferation and differentiation and can be therefore considered as new targets for cancer therapy (Arcangeli et al., 2009).

2. Materials and methods

2.1. Cell culture and treatments

Human hormone-sensitive breast adenocarcinoma cell line MCF-7 was obtained from American Type Culture Collection (ATCC, Manassas, VA, USA). The cells were cultured as previously described (Margheri et al., 2012). Briefly, cells were cultured in Dulbecco's modified Eagle's medium (DMEM, Sigma, Milan, Italy) supplemented with 10% Fetal Bovine Serum (FBS, Sigma), 100 U/mL penicillin–streptomycin and 1% L-glutamine 200 mM (Sigma) in a humidified 5% CO₂ atmosphere at 37 °C. This medium was suitable to allow cells growth/proliferation. In all the experiments melatonin 100 μM (Sigma) was used. This dose was proved to be the most effective to reduce cell viability and proliferation in this experimental model (Margheri et al., 2012). MCF-7 cells were cultured in growth medium in the presence of 100 μM melatonin for 24, 48, 72 h. In parallel experiments, the cells were cultured for 72 h in growth medium in the presence of melatonin and/or the following channel blockers (Sigma): nifedipine (10 μM) and NiCl₂ (50 μM) for L- and T-type Ca²⁺ channels; α-dendrotoxin, α-DTX (10 nM) for K_(V), iberiotoxin, IbTx (100 nM) for BK and chromanol, Chr (50 μM) for K_s channels. The treatments lasted up to 72 h and the media were daily replaced. In other experiments the cells were cultured for 72 h in differentiation medium (supplemented with 2% FBS) and treated with channel blockers as above described.

2.2. Cell growth/viability assay (MTS)

Cell growth/viability was evaluated by 3-(4,5-dimethylthiazol-2-yl)-5-(3-carboxymethoxyphenyl)-2-(4-sulfophenyl)-2Htetrazolium (MTS) assay (Promega, Madison, WI, USA). MCF-7 cells were plated into 96-multiwell-plates and then treated with melatonin 100 μM and/or the above-mentioned channel blockers for 72 h. Then, the cells were shifted in 100 μl of fresh medium phenol red-free and 20 μl of MTS test solution was added to each well. After 4 h of incubation, the color reaction was measured using a multi-well scanning spectrophotometer (Enzyme-Linked ImmunoSorbent Assay-ELISA- reader) (Amersham, Pharmacia Biotech, Cambridge, UK) at a wavelength of 490 nm. The values were expressed as mean ± S.D. obtained from five independent experiments carried out in triplicates.

In some experiments MCF-7 were treated with melatonin for 72 h in growth medium and, in a parallel set of experiments, in differentiation medium and treated with different channel blockers.

2.3. Confocal immunofluorescence

To detect proliferation activity, untreated and treated MCF-7 cells grown on glass coverslips were fixed with 0.5% buffered paraformaldehyde for 10 min at room temperature. After permeabilization with cold acetone for 3 min, the fixed cells were blocked with 0.5% bovine serum albumin (BSA; Sigma) and 3% glycerol in PBS for 20 min and then immunostained with rabbit polyclonal anti-Ki-67 (1:100; Abcam, Cambridge, UK). The immunoreaction was revealed by incubation with specific anti-rabbit Alexa Fluor 488-conjugated IgG (1:200; Molecular Probes, Eugene, OR, USA), for 1 h at room temperature. After washing in PBS, the sections were mounted with an anti-fade mounting medium (Biomedica Gel mount, Electron Microscopy Sciences, Foster City, CA, USA). A negative control was performed by replacing the primary antibody with non-immune mouse serum. Sections were examined with a Leica TCS SP5 confocal laser scanning microscope (Leica Microsystem, Mannheim, DE) equipped with a HeNe/Argon laser source for fluorescence measurements. Fluorescence was collected using a Leica PlanApo x63 oil-immersion objective. Optical sections (1024 × 1024 pixels) at intervals of 0.8 μm were obtained and superimposed to create a single composite image. When needed, a single optical fluorescent section and DIC images were merged to view the precise distribution of the immunostaining. Quantification of Ki-67 expression was performed on digitized images by counting the number of positive cells over the total cell number.

2.4. Confocal analysis of intracellular Ca²⁺ concentration

The analysis of [Ca²⁺]_i was performed as previously reported (Formigli et al., 2002). Briefly, to reveal the resting intracellular calcium concentration in MCF-7 cells in the absence or presence of melatonin (100 μM), ~2 × 10⁴ cells were plated on glass coverslips and incubated at 37 °C for 10 min in DMEM with Fluo 3-acetoxymethyl ester (Molecular Probes) as fluorescent Ca²⁺ indicator at a final concentration of 10 μM and 0.1% anhydrous dimethyl sulfoxide and Pluronic F-127 (0.01% wt/vol) as dispersing agent (Molecular Probes). After being washed, the cells were placed in open slide flow-loading chambers mounted on the stage of the confocal laser scanning microscope. Optical sections (1024 × 1024 pixels) at intervals of 0.8 μm were obtained. A variable number of cells ranging from 15 to 30 were analysed for each cell preparation. Multiple regions of interest (ROIs) of 25 μm² were selected within the cells to monitor Ca²⁺ signals, and outside the cells as baseline. Fluorescence signals were expressed as fractional changes above the resting baseline, ΔF/F, where F was the averaged baseline fluorescence and ΔF represented the fluorescence changes from the baseline.

2.5. Electrophysiological experiments

The electrophysiological characteristics of different voltage-gated ionic channels of cultured MCF-7 were investigated on glass coverslip-adherent single cells at room temperature (20–23 °C) by the whole-cell patch-clamp technique (Baglioni et al., 2009; Margheri et al., 2012); both voltage-clamp and current-clamp modes were used.

2.5.1. Solutions

Experiments performed to evaluate the membrane passive properties (membrane conductance, G_m , and cell capacitance, C_m) and resting membrane potential were carried out in Normal Tyrode bath solution with the following composition (mM): NaCl 140, KCl 5.4, CaCl_2 1.5, MgCl_2 1.2, glucose 5.5, and HEPES/NaOH 5 (pH 7.35). For K^+ and Ca^{2+} currents records we used a modified Normal Tyrode solution with different specific channels blockers added: TTX (1 μM) to block voltage activated Na^+ channels, 4-aminopyridine (2 mM) to block the 4-aminopyridine sensitive-transient outward potassium current (I_{to}) and BaCl_2 (0.4 mM) to block the inward rectifier K^+ current, I_{Kir} . To record only K^+ currents without any inward Ca^{2+} current contamination we added nifedipine (10 μM) and Ni^{2+} (50 μM) to block L- and T-type Ca^{2+} current, respectively or Cd^{2+} (0.8 mM) to block both the types. To evaluate the presence of the voltage- and Ca^{2+} -dependent delayed-rectifier iberitoxin-sensitive K^+ current (I_{BK}), of the slowly activating chromanol-sensitive K^+ current (I_{KS}) and of the fast activating α -dendrotoxin-sensitive K^+ current, $I_{K(V)}$, we performed a pharmacological dissection as previously reported (Baglioni et al., 2012). Briefly, we first applied the stimulation protocol in control condition to record the total K^+ current traces ($I_{K,tot}$). This was the result of the amount of all the three K^+ currents mentioned above plus a residual current (I_x), due to other currents that were not eliminated or not completely blocked by our procedure. After that, we generally applied the selective drugs in the following sequence: Chr, IbTx and α -DTX to block I_{KS} , I_{BK} and $I_{K(V)}$, respectively. After Chr application, the remaining currents were $I_{BK}+I_{K(V)}+I_x$; after Chr and IbTx application, $I_{K(V)}+I_x$ remained and, finally, after Chr, IbTx and α -DTX addition, only I_x remained. Subsequently, the current traces obtained in the presence of Chr were subtracted from those recorded in control condition to obtain the slowly activating I_{KS} current; then, the traces recorded in the presence of Chr and IbTx were subtracted from traces in Chr to assess the I_{BK} current time course. Finally, the traces recorded in the presence of Chr, IbTx and α -DTX were subtracted from Chr and IbTx traces to observe the fast activating $I_{K(V)}$ time course.

Experiments aimed to record only Ca^{2+} currents were performed in a high-TEA solution (Na^+ - and K^+ -free) (mM): CaCl_2 10, TEABr 145 and HEPES 10.

Patch pipettes had tip resistances of 3–7 $\text{M}\Omega$. For K^+ currents records, they were filled with a solution containing (mM): KCl 130, NaH_2PO_4 10, CaCl_2 0.2, EGTA 1, MgATP 5 and HEPES 10. pH was set to 7.2 with KOH. For Ca^{2+} currents records, the same kind of electrodes were filled with (mM): 150 CsBr, 5 MgCl_2 , 10 EGTA and 10 HEPES. pH was set to 7.2 with CsOH.

2.5.2. Stimulation protocols

The Ca^{2+} currents activation pulse protocol consisted of 1-s long step pulses applied to cells held at -80 mV and ranging from -70 to 50 mV in 10 mV increments. The protocol used an interval of 20 s between stimulating episodes for recovery. The steady-state inactivation was studied by a two-pulse protocol with 1-s pre-pulses to different voltages followed, after 500 ms, by 1-s test pulse fixed to -20 or 0 mV for T- and L-type Ca^{2+} currents, respectively. Again, in the two-pulse protocol, we used an interval of 10 s between stimulating episodes for recovery. All the activation and inactivation protocols were repeated twice. The steady-state ionic current activation was evaluated by: $I_a(V)=G_{\text{max}}(V-V_{\text{rev}})/\{1+\exp[(V_a-V)/k_a]\}$ and steady-state inactivation by: $I_h(V)=I/\{1+\exp[-(V_h-V)/k_h]\}$, where G_{max} is the maximal conductance for the I_a ; V_{rev} is the apparent reversal potential; V_a and V_h are the potentials eliciting the half-maximal activation and inactivation values, respectively; k_a and k_h are the steepness

factors. The passive properties parameters were evaluated as previously described (Baglioni et al., 2009). Linear leak and capacitive currents were canceled on-line using the P/4 procedure. This procedure also minimized the not-voltage dependent currents such as those flowing through intermediate-conductance Ca^{2+} -activated K^+ channels, IKCa (Haren et al., 2010), and stretch activated channels (Formigli et al., 2007; Sbrana et al., 2008).

The total K^+ current ($I_{K,tot}$) flowing through delayed rectifier channels was recorded in modified Normal Tyrode solution, evoked in voltage clamp mode by applying voltage steps in 10 mV increments from a holding potential (HP) of -80 mV. Moreover, to minimize Ca^{2+} currents that could counterbalance the outward K^+ currents we used an HP of -60 and -40 mV or, in some experiments, nifedipine and Ni^{2+} . To analyse the Ca^{2+} - and voltage- dependent K^+ current, I_{BK} , two procedures were used. First, the I_{BK} voltage-dependence in the MCF-7 cells was investigated as reported in Margheri et al. (2012). Then, the Ca^{2+} -dependence of I_{BK} was studied using a double-pulse protocol according to Prakriya and Lingle (1999) in modified Normal Tyrode solution with α -DTX (10 nM) and Chr (50 μM) added to block $I_{K(V)}$ and I_{KS} . In brief, the voltage command consisted of a double-pulse protocol with a test potential of 400 ms to 70 mV preceded by a pre-pulse to 0 mV. This test pulse to 70 mV allowed the I_{BK} occurrence without Ca^{2+} influx or with just a reduced one, since this voltage value is close to the Ca^{2+} reversal potential. The pre-pulse to 0 mV was used to activate the maximal inward Ca^{2+} currents. In order to evaluate the I_{BK} Ca^{2+} -dependence we increased the Ca^{2+} influx by increasing the pre-pulse duration. This was increased from 5 to 25 ms in 5 -ms increments and from 25 to 95 ms in 10 -ms increments.

The C_m value was considered as an index of the cell surface area assuming that membrane-specific capacitance is constant at 1 $\mu\text{F}/\text{cm}^2$. The total current amplitude (I_{tot}) of each type of channel investigated was used as an index of the total channel functionality, whereas current values normalized to cell linear capacitance (I/C_m) was referred to as current density. Current records were considered reliable when the rundown of C_m , resting membrane potential or the studied ionic current size was less than 5% .

2.6. Statistical analysis

Mathematical and statistical analysis of electrophysiological data was performed by pClamp9 (Axon Instruments) and Sigma-Plot (Jandel Scientific). The Kolmogorov–Smirnov test was used to verify normal distribution of the data. ANOVA was applied for multiple comparisons, followed by the Dunnett's post-hoc test. The number of cells used is indicated as n in figures and table legends. Data are expressed as the mean \pm S.E.M. Statistical significance was determined by one-way ANOVA and Newman–Keuls multiple comparison for analysis of cell growth/viability assay or Student's t test. A P value ≤ 0.05 was considered significant. Calculations were performed using GraphPad Prism software (GraphPad, San Diego, CA, USA).

3. Results

3.1. Melatonin reduces Ca^{2+} currents in MCF-7 cells

To estimate the effect of melatonin on ion currents known to have a role in cell proliferation, we firstly focused on T- and L-type Ca^{2+} currents. Since several studies demonstrated that human mammary cancer cell lines express voltage-dependent Ca^{2+} channels (Bertolesi et al., 2002; Ohkubo and Yamazaki, 2012), we intended to evaluate the effects of melatonin on voltage-dependent Ca^{2+} currents in MCF-7 cells cultured in growth medium. In control conditions we

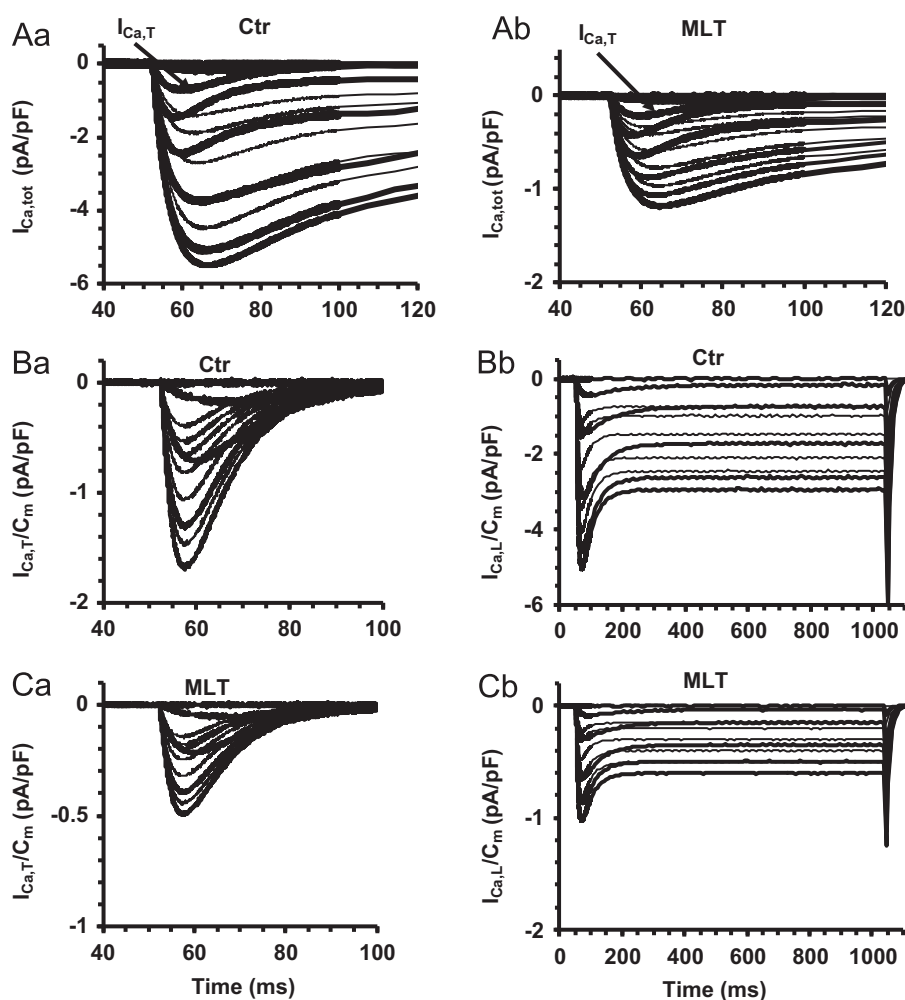


Fig. 1. Melatonin treatment affects Ca^{2+} current. Typical current traces recorded in high TEA- Ca^{2+} solution from a control and a melatonin-treated cell after 72 h in culture in growth medium. A) Typical total Ca^{2+} current traces, $I_{\text{Ca,tot}}$, evoked by voltage steps from -70 to 50 mV in 10 mV increments ($\text{HP} = -80$ mV), in the absence (Aa, Ctr) and in the presence of melatonin $100 \mu\text{M}$ (Ab, MLT). Ba) Representative family of $I_{\text{Ca,T}}$ current traces evaluated in a control cell in the presence of nifedipine $100 \mu\text{M}$; only the first 100 ms of the pulse are depicted for clarity to better observe the presence of the transient $I_{\text{Ca,T}}$. Bb) Representative family of $I_{\text{Ca,L}}$ current traces obtained by subtracting $I_{\text{Ca,T}}$ from the $I_{\text{Ca,tot}}$ traces. C) $I_{\text{Ca,T}}$ (a) and $I_{\text{Ca,L}}$ (b) from a melatonin-treated cell. Note the different ordinate scale between panels Ba and Ca, as well as Bb and Cb.

could observe a low voltage-activated inward transient current starting from -60 mV up to -40 mV. For further depolarizing voltage steps a slowly activating and decaying current superimposed on such a transient current (Fig. 1Aa). When nifedipine was added to the bath solution, only the transient response was recorded (Fig. 1Ba). This latter was no longer detectable when Ni^{2+} was added in the recording chamber (not shown), so we assumed it was $I_{\text{Ca,T}}$. Since no Ca^{2+} currents were observed in the presence of Ni^{2+} and nifedipine, we reasonably suppose that the only type of high voltage activated Ca^{2+} channel expressed on MCF-7 cells was the L-type one. Thus, the related L-type Ca^{2+} current was obtained by subtracting $I_{\text{Ca,T}}$ from the total I_{Ca} current (Fig. 1Bb). The resulting L-type Ca^{2+} current, $I_{\text{Ca,L}}$, generated by a 0 mV pulse peaked at about 20 ms and after an early fast inactivation with a time constant of about 20 ms, it was followed by a slowly decaying phase after about 200 – 250 ms having a time constant of about 280 ms.

Melatonin treatment was able to clearly reduce $I_{\text{Ca,tot}}$ size (Fig. 1Ab). In particular, we observed the decrease in amplitude of both Ca^{2+} current types (Fig. 1Ca and Cb) as compared to control cells. Moreover, the voltage eliciting the maximal peak current size was positively shifted of about 5 and 10 mV for $I_{\text{Ca,T}}$ and $I_{\text{Ca,L}}$, respectively (Table 1). Therefore, melatonin was able to shift the voltage dependence of $I_{\text{Ca,T}}$ and $I_{\text{Ca,L}}$ towards positive potentials.

Then, the mean peak current value estimated in all the experiments done was plotted vs. voltage (Fig. 2A). The analysis of the Boltzmann curves fitted to the normalized I - V data for activation and inactivation of both Ca^{2+} currents types (Fig. 2B and C), shows that melatonin positively shifted the V_a values for $I_{\text{Ca,T}}$ and $I_{\text{Ca,L}}$ activation of about 5 and 10 mV, respectively (Table 1). In contrast, we did not observe any significant shift of V_h neither for $I_{\text{Ca,T}}$ or $I_{\text{Ca,L}}$.

$I_{\text{Ca,L}}$ steady-state inactivation showed an U-shaped curve. Notably, the decaying branch at negative potentials was not affected by melatonin, but that at positive potentials was reduced (Fig. 2C).

Interestingly, by analysing the best fit to the resulting I - V curves we could clearly observe that the reversal potential was positively shifted in both the current types in a similar amount of about 8 mV (Fig. 2Aa and Ab, showed in detail in 2Ac; compare red triangles and blue circles related to melatonin vs. black symbols, related to Ctr). From the estimated value of the I_{Ca} reversal potential resulting in melatonin-treatment, we could suggest that melatonin may be able to induce a decrease of free $[\text{Ca}^{2+}]_i$. This assumption was confirmed by experiments of Ca^{2+} imaging showing that in melatonin-treated cells the resting $[\text{Ca}^{2+}]_i$ was actually reduced by about 50% with respect to control cells (Fig. 3).

3.2. Melatonin treatment affects different types of K^+ currents in MCF-7 cells

To test melatonin effects on K^+ currents in MCF-7 cells, we performed a detailed electrophysiological analysis. First, the

Table 1

MLT affects Boltzmann parameters of $I_{Ca,T}$ and $I_{Ca,L}$ activation and inactivation. MLT decreases the maximum peak size of $I_{Ca,T}$ and $I_{Ca,L}$, indexes of the inhibitory effect on these channels activity; moreover it shifts the voltage threshold and the voltage values eliciting the maximal peak current in the $I-V$ plots (V_p) and the V_a Boltzmann parameters of activation for both $I_{Ca,T}$ and $I_{Ca,L}$ towards more positive potentials. MLT did not affect the parameters k_a , k_h and V_h for both $I_{Ca,T}$ and $I_{Ca,L}$.

Parameters	Control	Melatonin
$I_{Ca,T}$		
$I_{Ca,T}/C_m$ (pA/pF)	1.7 ± 0.18	0.5 ± 0.12 ^a
G_m/C_m (pS/pF)	21.8 ± 2.00	6.2 ± 1.30 ^a
V_p (mV)	-30.1 ± 2.42	-25.2 ± 1.58 ^b
V_a (mV)	-40.1 ± 2.68	-35.0 ± 1.71 ^c
k_a (mV)	5.5 ± 0.43	5.5 ± 0.52
V_{rev} (mV)	58.0 ± 2.75	61.8 ± 2.78 ^c
V_h (mV)	-64.6 ± 4.06	-64.9 ± 3.10
k_h (mV)	4.5 ± 0.53	4.4 ± 0.42
$I_{Ca,L}$		
$I_{Ca,L}/C_m$ (pA/pF)	4.9 ± 0.38	2.0 ± 0.42 ^a
G_m/C_m (pS/pF)	88.0 ± 14.21	36.4 ± 10.24 ^a
V_p (mV)	0.24 ± 2.05	10.4 ± 3.08 ^a
V_a (mV)	-10.0 ± 2.09	-5.2 ± 1.06 ^a
k_a (mV)	7.2 ± 0.36	7.3 ± 0.47
V_{rev} (mV)	59.0 ± 2.76	68.2 ± 2.73 ^c
V_h (mV)	-55 ± 3.00	-52.5 ± 3.02
k_h (mV)	7.5 ± 0.46	7.4 ± 0.51

Data are mean ± S.E.M. and in each experimental condition were from $n=36/39$ cells.

^a $P < 0.005$ respect to control (Student's t -test).

^b $P < 0.01$.

^c $P < 0.05$.

different types of K^+ currents recorded were identified by a pharmacological dissection. After that, we performed the same experiments on melatonin-treated cells. A representative experiment related to cells cultured for 72 h in growth medium is reported in Fig. 4: it shows an example of pharmacological dissection of K^+ currents in a typical MCF-7 cell where only the current response to a 50-mV pulse is displayed, either in an untreated (Ctr) or in a melatonin-treated cell (MLT).

Representative currents elicited at any step potential are depicted as current density in Fig. 5 and referred to $I_{K,tot}$ (A), I_{BK} (B), I_{Ks} (C) and $I_{K(V)}$ (D) from untreated (panels a, Ctr) and melatonin-treated cells (panels b, MLT). It can be clearly seen that melatonin treatment caused a reduction in $I_{K,tot}$ density (Fig. 5Aa and Ab). Thanks to the pharmacological dissection (see Section 2), we could assess that such a decrease was mostly due to the strong decline of I_{BK} and $I_{K(V)}$ current density (about 0.3 and 0.4 fold, respectively, Fig. 5B and D). In contrast, melatonin treatment appeared to increase I_{Ks} current density (about 1.6 fold, Fig. 5C). The $I-V$ plots related to all the experimental data confirmed this conclusion (panels c).

3.3. Effect of melatonin treatment on I_{BK} Ca^{2+} -dependence

Due to the striking role likely played by I_{BK} in MCF-7 cells cultured in growth medium, we aimed to study in detail its Ca^{2+} -dependence. Thus, to evaluate the entity of melatonin effects on I_{BK} Ca^{2+} -dependence we applied the two-pulse protocol in MCF-7 cells (see Methods). I_{Ca} recorded by stepping the voltage to 0 mV in the absence and presence of Cd^{2+} (0.8 mM) is shown in Fig. 6A. In the absence of Cd^{2+} we recorded an inward current (I_{Ca}) followed by an outward one (I_{BK} , blue traces), that was completely blocked by Cd^{2+} (red traces). The effect of Ca^{2+} influx on I_{BK} was studied by pre-pulsing the membrane potential to 0 mV (Fig. 6). When the membrane potential was stepped from 0 mV to 70 mV the current traces showed an instantaneous current (I_{ist}) (Marcantoni et al., 2010;

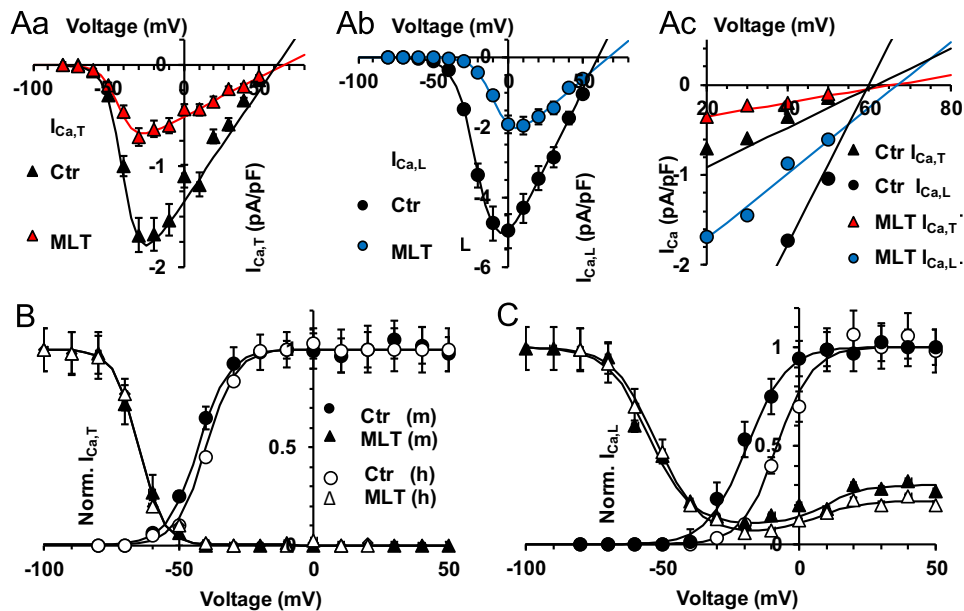


Fig. 2. The Voltage dependence of T- and L-type Ca^{2+} current is affected by melatonin. $I-V$ plots of T- ($I_{Ca,T}$) (Aa, black and red triangles are for Ctr and melatonin (MLT)-treated cells) and L-type Ca^{2+} currents ($I_{Ca,L}$) (Ab, black and blue circles are for Ctr and melatonin-treated cells, respectively) from experiments as in Fig. 1. (Ac) overall $I_{Ca}-V$ plots with different axes scale to better appreciate the shift of V_{rev} caused by melatonin respect to Ctr (symbols and colors as in panel Aa and Ab). (Aa-c) Single Boltzmann fits superimposed to the experimental data. (B and C) Related steady-state activation (m, circles) and inactivation (h, triangles) curves in control (filled symbols) and melatonin-treated cells (open symbols) for $I_{Ca,T}$ (B) and $I_{Ca,L}$ (C). (C) Note the U-shaped inactivation curve of $I_{Ca,L}$ for positive voltages; best fit to the data is obtained by the sum of two Boltzmann terms. All the data (mean values ± S.E.M.) are related to cells ($n=36/39$) cultured for 72 h. Boltzmann parameters, statistical analysis and number of analyzed cells are reported in Table 1. (For interpretation of the references to color in this figure legend, the reader is referred to the web version of this article.)

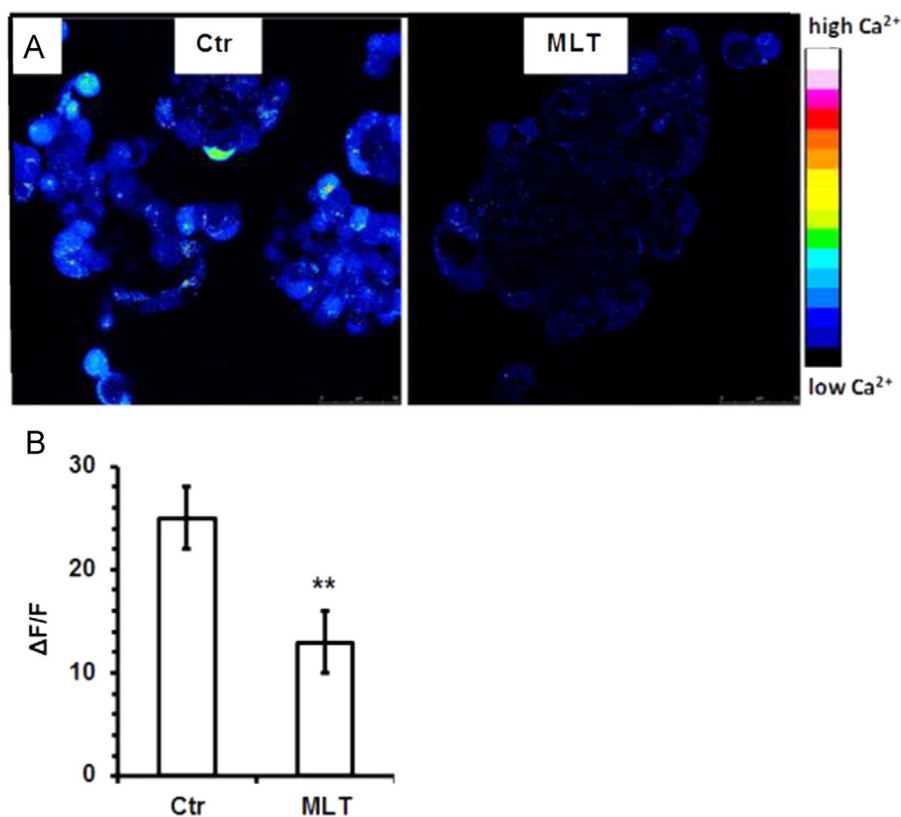


Fig. 3. Resting $[Ca^{2+}]_i$ is affected by melatonin. Confocal analysis of intracellular calcium concentration. (A) MCF-7 cells were treated without (Ctr) and with melatonin (MLT) 100 μ M for 72 h in growth medium. The pseudocolouring represents the absolute Ca^{2+} level as indicated by the color bar. (B) Fluorescence signals expressed as fractional changes $\Delta F/F$ in control (Ctr) and melatonin-treated cells. The values are expressed as mean \pm S.D. of five independent experiments carried out in triplicates. $^{**}P < 0.01$ of MLT vs. Ctr.

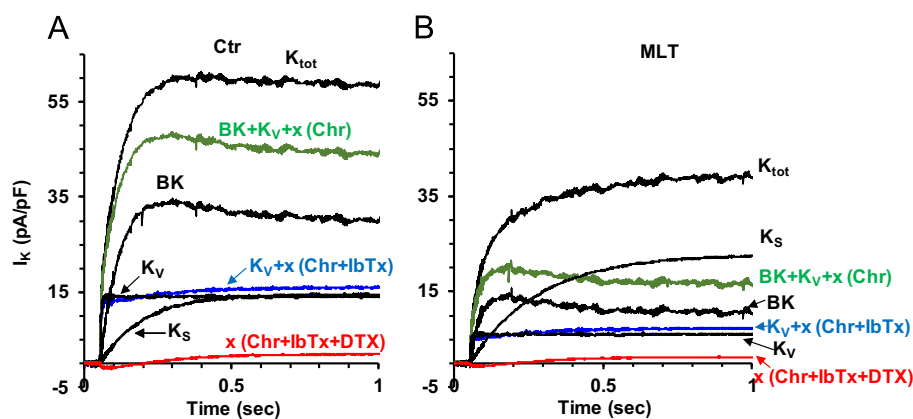


Fig. 4. Pharmacological dissection of K^+ currents. Typical total delayed rectifier K^+ current traces, $I_{K,tot}$ (upper black trace) elicited by a voltage step to 50 mV from $HP = -60$ mV in control solution (modified Normal Tyrode) with Nifedipine (10 μ M) and Ni^+ (50 μ M) in the absence (A) and in the presence of melatonin (B) recorded after 72 h in growth medium. $I_{K,tot}$ is the sum of I_{K_s} , I_{BK} , $I_{K(V)}$ and I_x currents. The single types of K^+ currents were dissected by adding specific blockers (see Section 2). For any colored trace, the channel blockers used are indicated in brackets next to the evoked current indication. In any panel, the single type of K^+ current was obtained by mathematical subtraction: $I_{BK} + I_{K(V)} + I_x$ (green trace), $I_{K(V)} + I_x$ (blue trace) and I_x (red trace). (For interpretation of the references to color in this figure legend, the reader is referred to the web version of this article.)

Prakriya and Lingle 1999) followed by a slow increase in the current size. The changes induced by conditioning steps on I_p and t_p were very small and not statistically significant respect to 5–10 ms control test pulse (without pre-pulse). However, as long as the pre-pulse duration increased, I_p progressively augmented (Fig. 6a), t_p , evaluated from the beginning of the 70-mV pulse, decreased (Fig. 6c) and the time constant of the decay became faster, changing from 210 ± 0.28 ms (without pre-pulse) to 112 ± 15 ms (with 75-ms pre-pulse). The I_p reached the maximal amplitude and the minimum t_p for 75-ms pre-pulse (Fig. 6a and c). The I_{BK} maximal size (I_p value)

elicited by a 75-ms pre-pulse increased 1.7 ± 0.2 fold ($n=7$) with respect to that evoked without the pre-pulse.

I_{BK} was then recorded in melatonin-treated cells cultured in growth medium for 72 h, by the two-pulse protocol and the same recording solutions used in untreated cells. The effects on t_p and time constant of the decay time-dependence were not statistically different from those observed in control (Fig. 6c) but the increase of I_p amplitude was smaller as long as the pre-pulse duration increased, reaching a quasi-steady state over 45-ms duration. In such an interval the increment was only 1.4 ± 0.2 ($n=7$). The

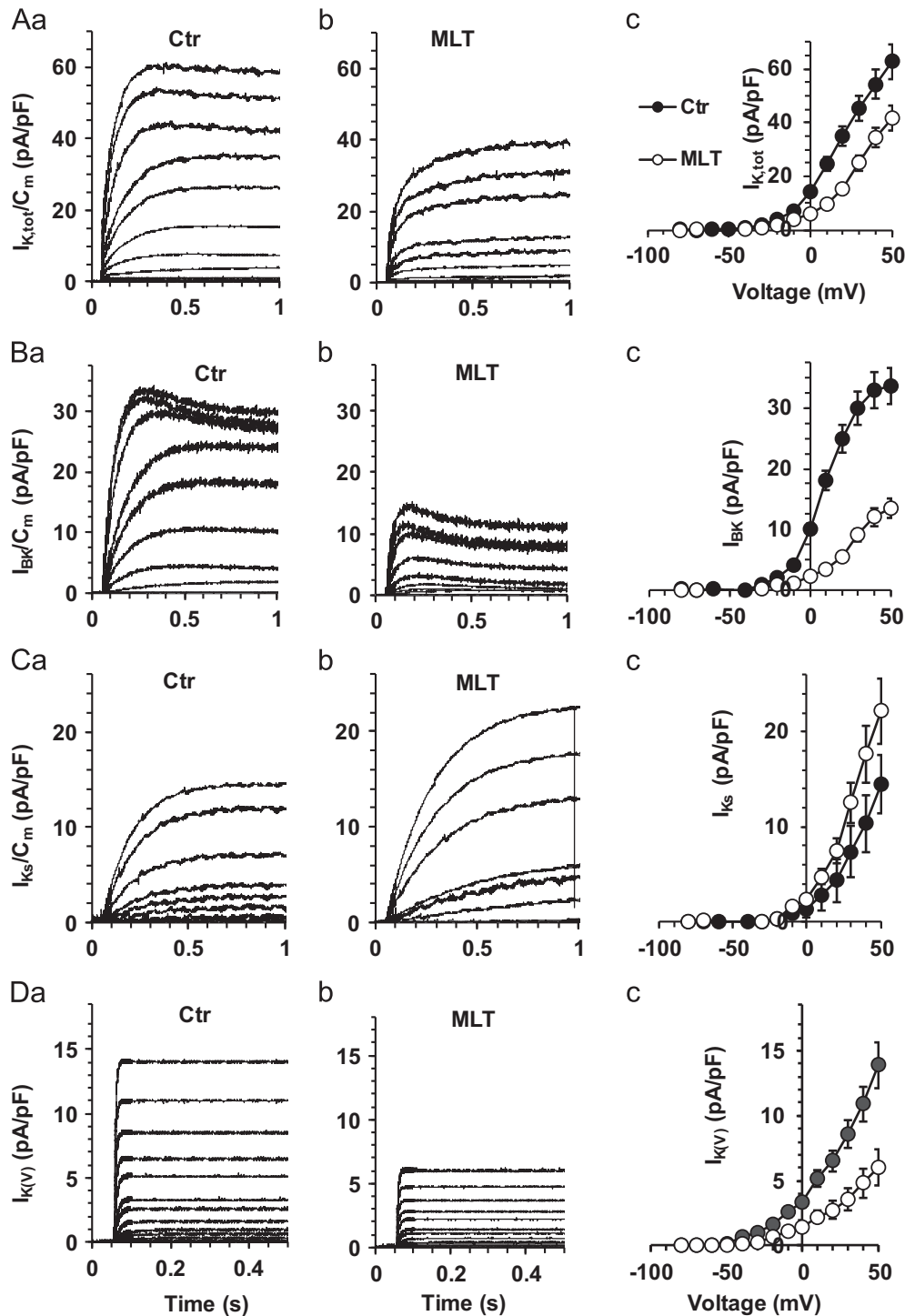


Fig. 5. Melatonin treatment affects different K^+ currents. $I_{K,tot}$ (A), I_{BK} (B), I_{Ks} (C) and $I_{K(V)}$ (D) family of current traces evaluated as in Fig. 4 (same cells and solutions) by pharmacological dissection with voltage steps in 10 mV-increments (from -80 to 50 mV); HP = -60 mV. K^+ currents from the control cells (a) and from the melatonin-treated cell (b). (c) I - V plots of normalized data (mean \pm S.E.M.) related to $I_{K,tot}$ (Ac), I_{BK} (Bc), I_{Ks} (Cc) and $I_{K(V)}$ (Dc) evaluated after 72 h in all control and melatonin-treated cells. Number of analyzed cells: Ctr $n=44$; melatonin $n=40$.

enhancement of I_{ist} occurred after 25 ms in control condition and after 45 ms under melatonin treatment. The I_{ist} enhancement in control was similar to I_p (1.6 ± 0.2) whereas it was reduced in melatonin-treated cells to 1.2 ± 0.1 ($P < 0.05$).

Finally, to test the role of $I_{Ca,T}$ on I_{BK} Ca^{2+} dependence we blocked $I_{Ca,L}$ with nifedipine. Since no difference was found between I_{BK} evaluated with and without pre-pulse (not shown), we suggest that T-type Ca^{2+} channels have a marginal role, if any, in modulating I_{BK} channels, possibly depending on the small

amount of Ca^{2+} entry due to its fast transient time course and small size, or because of their location too far from BK channels.

3.4. Melatonin affects MCF-7 cells proliferation and growth/viability

To confirm the previous finding on the effect of melatonin on proliferation on MCF-7 cells cultured in growth medium in the absence (control) or presence of melatonin for 72 h the nuclear levels of Ki-67, a well-known marker of cell cycle and proliferation

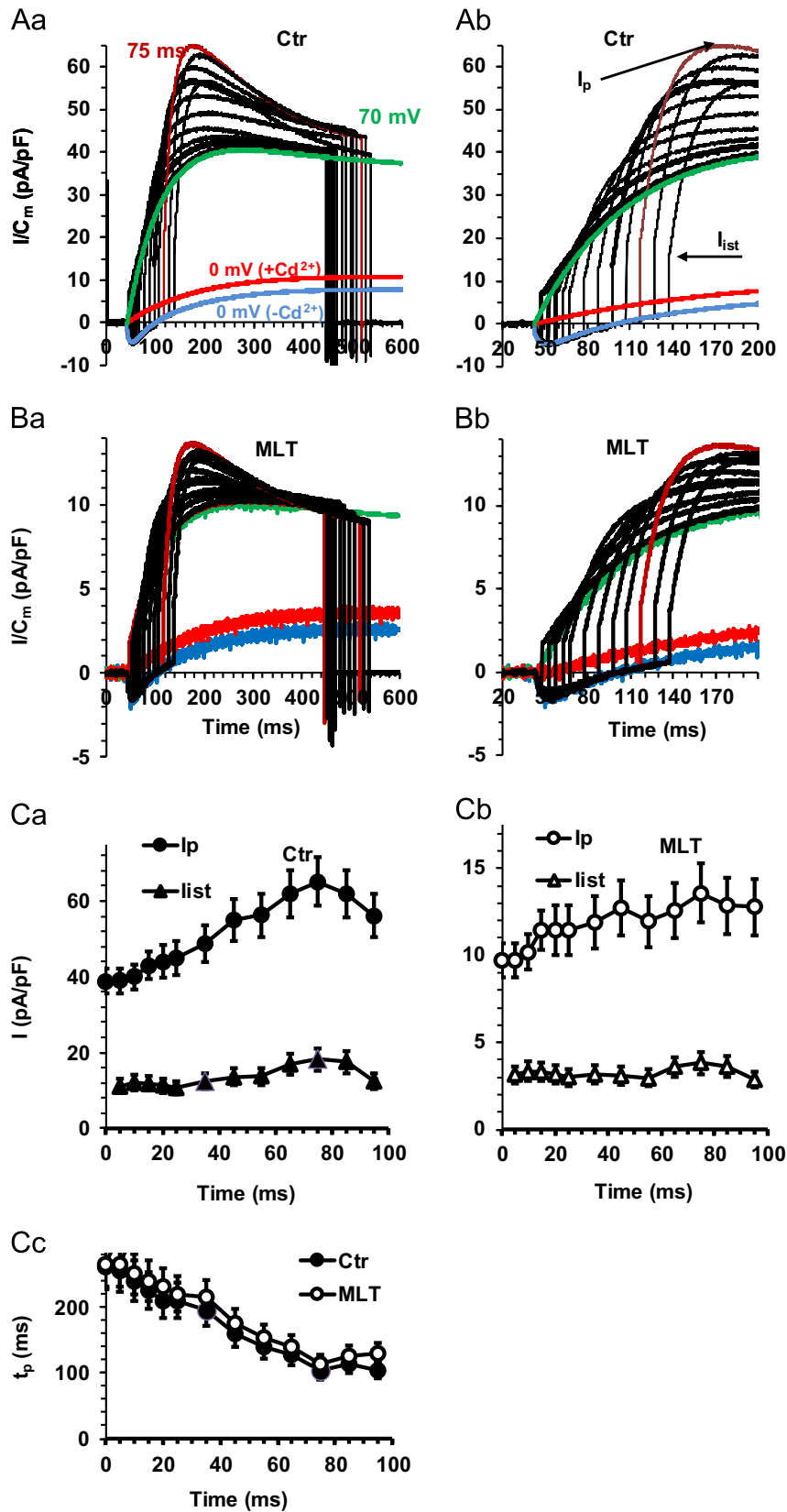


Fig. 6. Effect of melatonin on I_{BK} . Ca^{2+} -dependence of I_{BK} determined by the double pulse protocol in cells cultured in growth medium for 72 h without (A) and with melatonin (B). In each panel, the blue traces are elicited by a pulse to 0 mV (HP = -60 mV) and represent the sum of the inward I_{Ca} and the outward I_{BK} ; the red and green traces are the currents elicited by a pulse to 0 and 70 mV, respectively; the black traces are elicited by a pre-pulse to 0 mV of 5, 15, 20, 25, 35, 45, 55, 65, 75, 85 and 95 ms followed by a 400-ms long test pulse to 70 mV. The maximal enhancement of I_{BK} is obtained by a 75 ms-long prepulse (brown traces). (C) Enhancement of the maximal I_{BK} amplitude (I_p and I_{ist}) as a function of the pre-pulse duration in control (a) and after melatonin treatment (b). I_{ist} is the instantaneous current evoked when the membrane potential was stepped from 0 mV to 70 mV. Time to peak t_p (c) as a function of the pre-pulse duration in control and after melatonin treatment. (C) Time zero indicates the values recorded without the pre-pulse. (For interpretation of the references to color in this figure legend, the reader is referred to the web version of this article.)

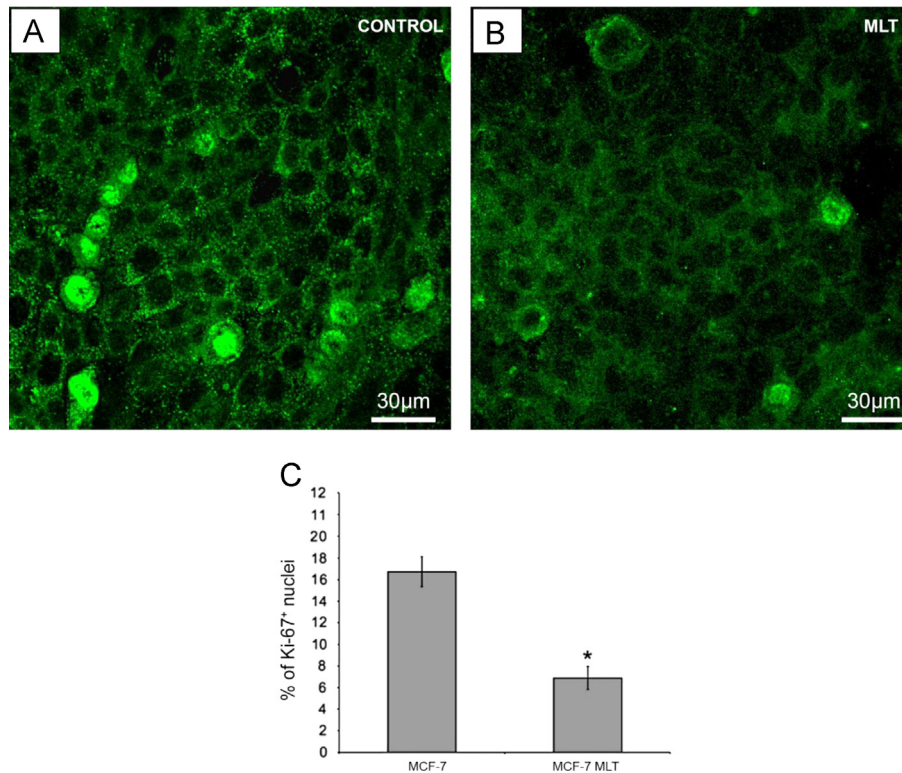


Fig. 7. Effects of melatonin on MCF-7 cell proliferation. Cells cultured in the absence (control) or presence of melatonin (MLT) 100 μ M for 72 h in growth medium (A and B, respectively). Cell proliferation estimated with polyclonal anti-Ki67 antibodies (green). C) The percentage of proliferating cells showing positive staining for Ki-67 nuclear antigen is shown in the histograms in control and melatonin-treated conditions. Values are expressed as mean \pm S.D. of five independent experiments carried out in triplicates. * $P < 0.05$ MLT vs. Ctr. (For interpretation of the references to color in this figure legend, the reader is referred to the web version of this article.)

were evaluated. Once more it was confirmed that the proliferating cells under melatonin treatment were reduced to about 40% with respect to the untreated ones (Fig. 7A–C). To assess MCF-7 cell growth/viability in growth medium, MTS assay revealed that melatonin was able to induce a statistically significant decline of growth/viability with respect to untreated cells (Fig. 8). The selective ion channel block (Fig. 8) by Nifedipine, NiCl_2 , α -DTX, IbTx, or Chr caused a slight but statistically significant inhibition of the cell growth/viability investigated by MTS assay with respect to control cells, indicating a significant role of the specific ion currents $I_{\text{Ca,L}}$, $I_{\text{Ca,T}}$, $I_{\text{K(V)}}$, I_{BK} and I_{Ks} in cell proliferation. The concomitant administration of melatonin with Nifedipine, NiCl_2 or IbTx did not induce significant changes with respect to control cells. These results seem to suggest that melatonin is unable to induce a growth/viability decrease through a pathway involving $I_{\text{Ca,L}}$, $I_{\text{Ca,T}}$ and I_{BK} . Nevertheless, melatonin further decreased cell growth/viability in the cells pre-treated with α -DTX or with Chr, indicating that, even if $I_{\text{K(V)}}$ or I_{Ks} are blocked, it can still exert its effect of reducing cell growth/viability. Therefore, it seems that the further reduction observed with melatonin in the presence of α -DTX or Chr may not strictly depend only on $\text{K}_{\text{(v)}}$ or K_{s} channels.

3.5. Effects of melatonin on C_m , resting membrane potential and ionic currents

The effects of melatonin in proliferating MCF-7 cells cultured in growth medium were estimated also at different culture times. Records in normal Tyrode solution on control MCF-7 cells cultured for 24, 48 and 72 h in growth medium showed a progressive increase in C_m , suggesting that cells underwent an increase in cell surface area; in contrast, in melatonin-treated cells C_m was scarcely affected since at 72 h it showed a slight and not significant decreased value as compared to the one observed at 24 h (Fig. 9A).

By using the current-clamp mode we also recorded the resting membrane potential of MCF-7 cells in normal Tyrode solution (Fig. 9B). It was observed that resting membrane potential tended to depolarize with time in untreated cells, whereas in melatonin-treated ones, it resulted always significantly hyperpolarized with respect to control, although this effect was stronger at 24 and 48 h, as compared to 72 h.

In control cells, the time-dependent increase of C_m was paralleled by the enhancement of the maximal values of current density and total current amplitudes of I_{BK} , I_{Ks} and $I_{\text{K(V)}}$ (Fig. 9C–E) and of Ca^{2+} currents ($I_{\text{Ca,T}}$ and $I_{\text{Ca,L}}$) (Fig. 9F and G). The effects of melatonin treatment on the various types of ion currents according to the culture time were similar. In fact, the time dependent enhancement was generally reduced and the total current values were decreased with respect to those observed in control. A similar trend was observed for Ca^{2+} current density. Except for K_{s} , melatonin did not affect the current density and total current amplitudes recorded at 24 h, showing the same mean size as in control, but it strongly decreased the ionic currents at 48 h and even more at 72 h (Fig. 9E G). Differently, I_{Ks} current density in the presence of melatonin was larger than control and increased with time in culture (Fig. 9Da). Moreover, K_{s} was the only component whose total current was increased in time in the presence of melatonin (Fig. 9Db), although its size was lesser than Ctr. This indicates that melatonin effect observed on I_{Ks} density was essentially related to the decrease of C_m .

3.6. Effects of melatonin on cells cultured in differentiation medium

To verify whether the effect of melatonin was expressing solely on proliferating cells, parallel experiments in MCF-7 cells cultured in differentiation medium, namely DMEM supplemented with a low serum concentration (FBS 2%). MTS assay to detect growth/viability

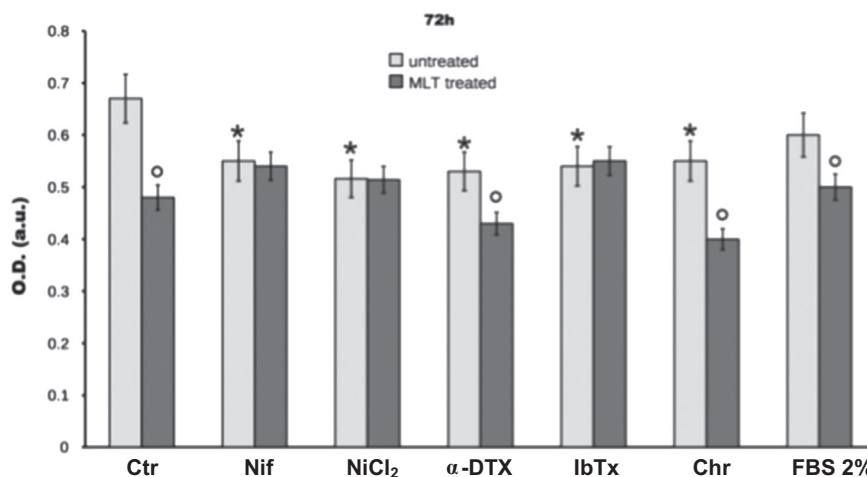


Fig. 8. Effects of melatonin, alone or in combination with different Ca^{2+} and K^{+} channel blockers, on MCF-7 cell growth/viability. MCF-7 cells, cultured in growth medium (DMEM supplemented with 10% FBS, Ctr), for 72 h were not treated (untreated) or treated with melatonin, 100 μM (MLT treated) and evaluated by MTS assay without or with the following channel blockers: nifedipine (10 μM) and NiCl_2 (50 μM) for L- and T-type Ca^{2+} channels, respectively; α -DTX (10 nM) for $\text{K}_{(\text{V})}$; IbTx (100 nM) for BK and Chr (50 μM) for K_s channels. Last pair of bars: cells were cultured in differentiation medium, that is DMEM supplemented with 2% FBS for 72 h. Values are expressed as mean \pm S. D. of five independent experiments carried out in triplicates. Optical density (O.D.) expressed in arbitrary units (a.u.). * $P < 0.05$ channel blockers in untreated vs. control; $^{\circ}P < 0.05$ FBS 2% vs. Ctr10%; $^{\circ}P < 0.05$ MLT treated vs. related untreated.

in MCF-7 cells cultured in differentiation medium (Fig. 8) revealed, as expected, a moderate reduction of cell growth/viability compared to the cells maintained in growth medium (indicated as Ctr in Fig. 8). The addition of melatonin significantly reduced growth/viability in differentiating cells, but its effect, in terms of variability reduction was less marked than that exerted on the cells cultured in growth medium (Ctr) suggesting that melatonin as a more marked effect on proliferation rather than on differentiation. After 72 h in culture, cells grown in differentiation medium ($n=22$) showed a smaller C_m as compared to control (Fig. 9A, filled diamond), indicating a decrease in surface area with respect to 24 h. The presence of melatonin ($n=20$) elicited an opposite effect, inducing a C_m increase (open diamond) vs. melatonin treatment in growth medium (open circles). However, this increase in cell surface area did not differ significantly from C_m value estimated in untreated cells after 24 h in growth medium (filled circle). Moreover, differentiating cells also showed a hyperpolarized resting membrane potential, typical of cells with slow proliferation rate; melatonin caused a further hyperpolarization (Fig. 9B, filled and open diamond, respectively).

The electrophysiological records performed on MCF-7 cells cultured for 72 h in differentiation medium (filled diamond), showed a reduction of the total current size of all the delayed rectifying outward currents (I_{BK} , I_{Ks} , $I_{\text{K(V)}}$) with respect to those cultured in growth medium at the same time (Fig. 9Cb, Db, and Eb, compare filled diamond with filled circles at 72 h). Thus, it can reasonably suggested that these currents have a prevalent role in proliferation. This effect was accompanied by a slight reduction of the calculated current density except for I_{Ks} that, in contrast, showed an increase (Fig. 9Ca, Da, and Ea, filled diamond). Similarly, the current density of $I_{\text{Ca,T}}$ and $I_{\text{Ca,L}}$ was strongly augmented (Fig. 9Fa and Ga), whereas the related total currents amplitudes were slightly increased after 72 h (Fig. 9Fb and Gb) with respect to cells grown in growth medium, thus suggesting a role for these channels also in differentiation.

Upon melatonin treatment, the total current values of I_{BK} and I_{Ks} recorded from cells in differentiation medium (Fig. 9Cb and Db, open diamond) were not significantly different respect to those observed at the same time in growth medium (open circles). By contrast, differently to what observed in growth medium, the total current values of $I_{\text{K(V)}}$ (Fig. 9Eb) as well as $I_{\text{Ca,T}}$ and $I_{\text{Ca,L}}$ (Fig. 9Fb and Gb) were increased. Since the mean total current amplitude of I_{BK} , $I_{\text{Ca,T}}$ and $I_{\text{Ca,L}}$ in the presence of melatonin in 2% FCS medium was

definitely lower than that detected in untreated cells (compare open and filled diamonds in Fig. 9Cb, Fb and Gb). Since I_{Ks} and $I_{\text{K(V)}}$ showed similar values in the presence or absence of melatonin in differentiation medium (compare open and filled diamonds in Fig. 9Db and Eb) it appears reasonable that melatonin has not detectable effects on these channels in the course of differentiation, but only upon proliferation. A similar effect was observed also on $I_{\text{K(V)}}$ current density where only a slight reduction could be seen (Fig. 9Ea), whereas I_{Ks} current density was sharply decreased (Fig. 9Da). AS for the current density of all other ion currents I_{BK} , I_{Ks} , $I_{\text{Ca,T}}$ and $I_{\text{Ca,L}}$ melatonin caused a significant decrease with respect to untreated cells (Fig. 9Ca, Da, Fa, and Ga) suggesting that melatonin may affect these channels functionality also in the process of differentiation.

4. Discussion

Different types of human cancers display a peculiar biophysical profile and/or atypical ionic channels activity. This is the reason why the role of ionic channels in the control of the cell cycle in normal and transformed cells has already been addressed by many research groups, in the attempt of identifying efficient targets for therapeutic approaches (Abdul et al., 2003; Arcangeli et al., 2009; Asher et al., 2010; Aydar et al., 2009; Becchetti, 2011; Currò, 2014; Wang, 2004). The detailed electrophysiological analysis performed in this study on MCF-7 cells adds new insights to the elucidation of the possible mechanisms involved in the oncostatic action of melatonin based on the cultured condition. Particularly, MCF-7 cells cultured for 72 h in growth medium had a reduced surface area, were more depolarized, and had a reduced $I_{\text{Ca,T}}$ and $I_{\text{Ca,L}}$, a greater I_{Ks} and a similar $I_{\text{K(V)}}$ and I_{BK} current density respect to MCF-7 cells cultured in differentiation medium.

The increase of the membrane depolarization, of the membrane surface and of all the voltage-dependent Ca^{2+} and K^{+} currents observed in the present study in control cells in growth medium suggests a progressive increase in the expression/activity of these channels along with culture time. This event can successfully maintain the proliferative potential of MCF-7 cells that is, one of the alarming features of the cancerous phenotype. When the cells were cultured in growth medium in the presence of melatonin, a significant reduction of proliferation and viability was observed as

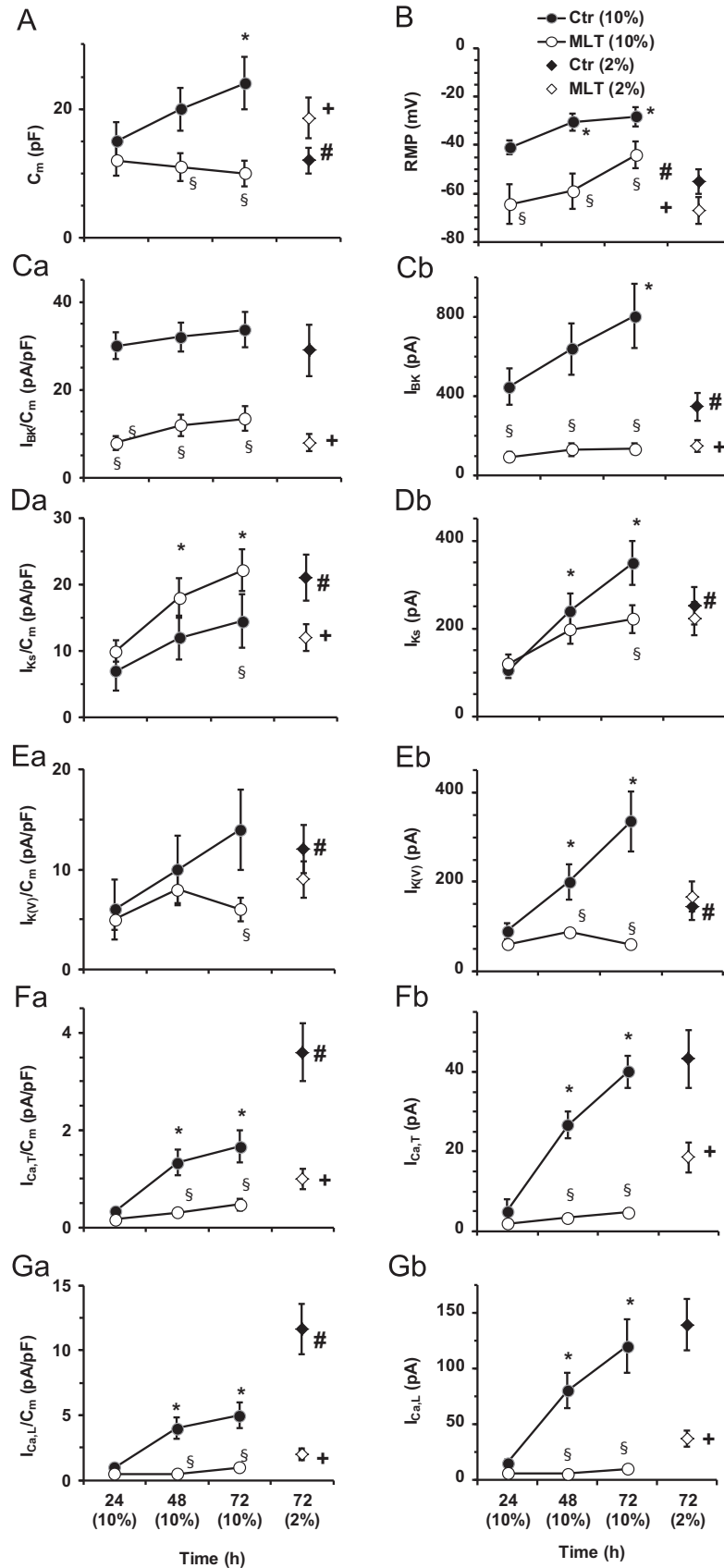


Fig. 9. Effects of melatonin on C_m , resting membrane potential (RMP) and maximal size of K^+ and Ca^{2+} currents with time in culture. C_m , resting membrane potential and maximal size of K^+ and Ca^{2+} currents were evaluated in untreated and melatonin-treated cells after 24, 48 and 72 h in growth medium (10%) and after 72 h in differentiation medium (2%). Cell capacitance C_m (A), resting membrane potential, RMP (B), I_{BK} (C), I_{Ks} (D), $I_{K(V)}$ (E), $I_{Ca,T}$ (F) and $I_{Ca,L}$ (G). C–G: Left panels (a) report K^+ and Ca^{2+} current density (in pA/pF) and right panels (b) the total currents (in pA). For cell cultured in 10% FBS: * $P < 0.05$ respect to the corresponding data at 24 h; § $P < 0.05$ of melatonin-treated cells respect to the corresponding data of Ctr. For cell cultured in 2% FBS: + $P < 0.05$ respect to the corresponding data at 72 h in 10% of FBS; # $P < 0.05$ of melatonin-treated respect to the corresponding untreated. The number of the cells investigated was $n = 44$ and 40 for Ctr and MLT (cells cultured in 10% FBS), $n = 24$ and 22 for Ctr and MLT (in 2% FBS).

compared to untreated ones. Actually, melatonin was able to reduce proliferation also in differentiating cells, but since this effect was less marked than that observed in cells cultured in growth medium a more effective action of melatonin on growth rather than on differentiation can be suggested. To verify this hypothesis the possible effects of melatonin on the different ion currents known to have a role in proliferation were tested.

In relation to I_{Ca} , our findings demonstrate that melatonin treatment was able to reduce both T- and L-type Ca^{2+} current amplitude and to provoke an alteration of the current voltage dependence along with a decrease of intracellular Ca^{2+} concentration. Since Ca^{2+} seems to be a crucial regulator of the cell cycle necessary for proper proliferation (Bertolesi et al., 2002; Gray et al., 2004; Naziroğlu et al., 2012; Wang et al., 2000), the associated reduction of free $[Ca^{2+}]_i$ observed in our experiments supports the clue that melatonin may contribute to the decline of proliferation also disturbing internal Ca^{2+} homeostasis. The G-protein-coupled melatonin MT1 receptors are expressed in MCF-7 cells (Girgert et al., 2009; Hill et al., 2011b; Jablonska et al., 2013; Jawed et al., 2007; Rich et al., 1999) and, via the inhibition of adenylate cyclase activity (Jablonska et al., 2013; Jawed et al., 2007), their activation leads to the decrease of adenosine 3', 5'-cyclic monophosphate (cAMP) synthesis. Considering that in MCF-7 melatonin affected cell functionality by a significant depletion of ATP levels (Margheri et al., 2012), we propose that the decrease of cAMP, leading to a decrease of PKA activity and channel phosphorylation, can be considered a crucial mechanism involved in the reduction of L- and T-type Ca^{2+} currents (Mahapatra et al., 2012; Novara et al., 2004; Sundelacruz et al., 2009), further stressing the evidence that Ca^{2+} channels are a target by which melatonin can modulate cell proliferation.

Similarly, in this study we demonstrated that also K^+ currents are involved in the melatonin modulatory action of cell proliferation. Melatonin treatment caused a reduction in $I_{K(v)}$ and I_{BK} but an increase of I_{Ks} density. MTS assay showed that melatonin decreased cell growth/viability in cells pre-treated with α -DTX or with Chr. However, this reduction may not univocally depend only on $K(v)$ or Ks channels, because even if such channels are blocked, melatonin can still exert its effect of reducing cell proliferation/viability through a pathway involving I_{BK} . BK channel activation requires Ca^{2+} entry which, in turn, activates BK channels located in close vicinity to the Ca^{2+} source (Berkefeld et al., 2006; Marcantoni et al., 2010). According to Berkefeld et al. (2006) and Marcantoni et al. (2010), our results on I_{BK} could be explained suggesting that melatonin was able to cause the shift of BK channels far from L-type Ca^{2+} channels, leading to the impairment of BK channels assembly and functionality and thus to the reduction of I_{BK} and its kinetics.

The depolarization of resting membrane potential is usually detected in proliferating cells and, since there is a clear correlation between resting membrane potential and mitotic activity, it is obvious that the maintenance of a proper membrane potential during cell cycling, mainly controlled by K^+ channels (Klimatcheva and Wonderlin, 1999), is of primary importance. The mean resting membrane potential values recorded in MCF-7 cells were quite depolarized, as typically observed in cancer cells with respect to that of terminally differentiated cells (Sundelacruz et al., 2009) and tended to depolarize further with time in culture. Whatever the mechanism underlying the establishment and the maintenance of resting membrane potential in cells cultured in growth medium, it can be affirmed that melatonin was capable to hyperpolarize the resting membrane potential which, conversely tended to depolarize with time in control condition. The hyperpolarization induced by melatonin can be partly justified by the L-type Ca^{2+} current decrease in amplitude, the increase of $[Ca^{2+}]_i$ and of I_{Ks} density.

However, to elucidate this issue, it must be considered that besides the voltage dependent ion channel activation, many other

mechanisms may contribute to the establishment of resting membrane potential, such as stretch activated channels (Aydar et al., 2009; Formigli et al., 2007; Sbrana et al., 2008), ionic pumps ($2Na/3K$ ATPase and Ca^{2+} pump), $3Na/Ca$ exchanger (Becchetti 2011) and voltage-independent channels as IKCa and K_{ATP} (Abdul et al., 2003; Blackiston et al., 2009; Haren et al., 2010; Klimatcheva and Wonderlin, 1999), and that the complexity of the scenario requires further investigations.

Moreover, melatonin reduced the increase of C_m that is usually observed in untreated-cells with time in culture. Therefore, we suggest that the increase of cell membrane surface area usually observed in control proliferating cells was definitely inhibited by melatonin, this effect being specifically addressed to cells in proliferation. In fact, when cells were cultured in differentiation medium, melatonin caused an increase in C_m . Moreover, data obtained by MTS assay showed that melatonin had a lower effect in reducing growth/viability in cells cultured in differentiation with respect to growth medium. Consequently, melatonin action differed according to the culture media and associated proliferation rate.

5. Conclusions

Our research shows that the alteration in ion channel gating may be considered as a final effector of the action of melatonin on cell proliferation. Even if this is just an *in vitro* study, it extends and provides novel experimental evidence related to the melatonin oncostatic action. In fact, the present findings indicate that melatonin is able to counteract proliferation as well as differentiation in MCF-7 cell line. This result strongly indicates that melatonin, as a modulator of different voltage-dependent ion channels, might act as a new promising tool for specifically disrupting cell viability and differentiation pathway in tumour cells and consequently may be potentially helpful in cancer therapy.

Acknowledgments

This paper is dedicated to the dear memory of Lucia Formigli who has passed away on March 18th, 2014. The authors wish to thank Dr D. Nosi for his valuable assistance in Ca^{2+} imaging experiments. This study was supported by LOGO-BIOS, O.N.L.U.S. Foundation 20100-m3810.

References

- Abdul, M., Santo, A., Hoosein, N., 2003. Activity of potassium channel-blockers in breast cancer. *Anticancer Res.* 23, 347–351.
- Arcangeli, A., Crociani, O., Lastraioli, E., Masi, A., Pillozzi, S., Becchetti, A., 2009. Targeting ion channels in cancer: a novel frontier in antineoplastic therapy. *Curr. Med. Chem.* 16, 66–93.
- Asher, V., Sowter, H., Shaw, R., Bali, A., Khan, R., 2010. Eag and HERG potassium channels as novel therapeutic targets in cancer. *World J. Surg. Oncol.* 29, 113–117.
- Aydar, E., Yeo, S., Djamgoz, M., Palmer, C., 2009. Abnormal expression, localization and interaction of canonical transient receptor potential ion channels in human breast cancer cell lines and tissues: a potential target for breast cancer diagnosis and therapy. *Cancer Cell Int.* 18, 9–23.
- Baglioni, S., Francalanci, M., Squecco, R., Lombardi, A., Cantini, G., Angeli, R., Gelmini, S., Guasti, D., Benvenuti, S., Annunziato, F., Bani, D., Liotta, F., Francini, F., Perigli, G., 2009. Characterization of human adult stem cell population isolated from visceral and subcutaneous adipose tissue. *FASEB J.* 23, 3494–3505.
- Baglioni, S., Cantini, G., Poli, G., Francalanci, M., Squecco, R., Di Franco, A., Borgogni, E., Frontera, S., Nesi, G., Liotta, F., Lucchese, M., Perigli, G., Francini, F., Forti, G., Serio, M., Luconi, M., 2012. Functional differences in visceral and subcutaneous fat pads originate from differences in the adipose stem cell. *PLoS One* 7, e36569.
- Becchetti, A., 2011. Ion channels and transporters in cancer. 1. Ion channels and cell proliferation in cancer. *Am. J. Physiol. Cell. Physiol.* 301, C255–C265.
- Berkefeld, H., Sailer, C.A., Bildl, W., Rohde, V., Thumfart, J.O., Eble, S., Klugbauer, N., Reisinger, E., Bischofberger, J., Oliver, D., Knaus, H.G., Schulte, U., Fakler, B., 2006. BKCa-Cav channel complexes mediate rapid and localized Ca^{2+} -activated K^+ signaling. *Science* 314, 615–620.

- Bertolesi, G.E., Shi, C., Elbaum, L., Jollimore, C., Rozenberg, G., Barnes, S., Kelly, M.E., 2002. The Ca^{2+} channel antagonists mibefradil and pimozide inhibit cell growth via different cytotoxic mechanisms. *Mol. Pharmacol.* 62, 210–219.
- Bielanska, J., Hernández-Losa, J., Pérez-Verdaguer, M., Moline, T., Somoza, R., Ramón y Cajal, S., Condom, E., Ferreres, J.C., Felipe, A., 2009. Voltage-dependent potassium channels Kv1.3 and Kv1.5 in human cancer. *Curr. Cancer Drug Targets* 9, 904–914.
- Blackiston, D.J., McLaughlin, K.A., Levin, M., 2009. Bioelectric controls of cell proliferation: ion channels, membrane voltage and the cell cycle. *Cell Cycle* 8, 3519–3528.
- Cos, S., Sánchez-Barceló, E.J., 2003. Melatonin and mammary pathological growth. *Front. Neuroendocrinol.* 21, 133–170.
- Currò, D., 2014. K^+ channels as potential targets for the treatment of gastrointestinal motor disorders. *Eur. J. Pharmacol.* 733, 97–101.
- Enomoto, K., Cossu, M.F., Maeno, T., Edwards, C., Oka, T., 1986. Involvement of the Ca^{2+} -dependent K^+ channel activity in the hyperpolarizing response induced by epidermal growth factor in mammary epithelial cells. *FEBS Lett.* 203, 181–184.
- Formigli, L., Francini, F., Meacci, E., Vassalli, M., Nosi, D., Quercioli, F., Tiribilli, B., Bencini, C., Piperio, C., Bruni, P., Orlandini, S.Z., 2002. Sphingosine 1-phosphate induces Ca^{2+} transients and cytoskeletal rearrangement in C2C12 myoblastic cells. *Am. J. Physiol. Cell Physiol.* 282, C1361–C1373.
- Formigli, L., Meacci, E., Sassoli, C., Squecco, R., Nosi, D., Chellini, F., Naro, F., Francini, F., Zecchi-Orlandini, S., 2007. Cytoskeleton/stretch-activated ion channel interaction regulates myogenic differentiation of skeletal myoblasts. *J. Cell. Physiol.* 211, 296–306.
- Gamper, N., Fillon, S., Huber, S.M., Feng, Y., Kobayashi, T., Cohen, P., Lang, F., 2002. IGF-1 up-regulates K^+ channels via PI3-kinase, PDK1 and SGK1. *Pflug. Arch.* 443, 625–634.
- Girgert, R., Hanf, V., Emons, G., Gründker, C., 2009. Membrane-bound melatonin receptor MT1 down-regulates estrogen responsive genes in breast cancer cells. *J. Pineal Res.* 47, 23–31.
- Grant, S.G., Melan, M.A., Latimer, J.J., Witt-Enderby, P.A., 2009. Melatonin and breast cancer: cellular mechanisms, clinical studies and future perspectives. *Expert Rev. Mol. Med.* 11, e5. <http://dx.doi.org/10.1017/S1462399409000982>.
- Gray, L.S., Perez-Reyes, E., Gomora, J.C., Haverstick, D.M., Shattock, M., McLatchie, L., Harper, J., Brooks, G., Heady, T., Macdonald, T.L., 2004. The role of voltage gated T-type Ca^{2+} channel isoforms in mediating “capacitative” Ca^{2+} entry in cancer cells. *Cell Calcium* 36, 489–497.
- Haren, N., Khorsi, H., Faouzi, M., Ahidouch, A., Sevestre, H., Ouadid-Ahidouch, H., 2010. Intermediate conductance Ca^{2+} activated K^+ channels are expressed and functional in breast adenocarcinomas: correlation with tumour grade and metastasis status. *Histol. Histopathol.* 25, 1247–1255.
- Hill, S.M., Blask, D.E., Xiang, S., 2011a. Melatonin and associated signaling pathways that control normal breast epithelium and breast cancer. *J. Mammary Gland Biol. Neoplasia* 16, 235–245.
- Hill, S.M., Cheng, C., Yuan, L., Mao, L., Jockers, R., Dauchy, B., Frasch, T., Blask, D.E., 2011b. Declining melatonin levels and MT1 receptor expression in aging rats is associated with enhanced mammary tumor growth and decreased sensitivity to melatonin. *Breast Cancer Res. Treat.* 127, 91–98.
- Hill, S.M., Frasch, T., Xiang, S., Yuan, L., Duplessis, T., Mao, L., 2009. Molecular mechanisms of melatonin anticancer effects. *Integr. Cancer Ther.* 8, 337–346.
- Jablonska, K., Pula, B., Zemla, A., Owczarek, T., Wojnar, A., Rys, J., Ambicka, A., Podhorska-Okolow, M., Ugorski, M., Dziegiel, P., 2013. Expression of melatonin receptor MT1 in cells of human invasive ductal breast carcinoma. *J. Pineal Res.* 54, 334–345.
- Jawed, S., Kim, B., Ottenhof, T., Brown, G.M., Werstki, E.S., Niles, L.P., 2007. Human melatonin MT1 receptor induction by valproic acid and its effects in combination with melatonin on MCF-7 breast cancer cell proliferation. *Eur. J. Pharmacol.* 560, 17–22.
- Jung, B., Ahmad, N., 2006. Melatonin in cancer management: progress and promise. *Cancer Res.* 66, 9789–9793.
- Klimatcheva, E., Wonderlin, W.F., 1999. An ATP-sensitive $K(+)$ current that regulates progression through early G1 phase of the cell cycle in MCF-7 human breast cancer cells. *J. Membr. Biol.* 171, 35–46.
- Kunzelmann, K., 2005. Ion channels and cancer. *J. Membr. Biol.* 205, 159–173.
- Lang, F., Henke, G., Embark, H.M., Waldegger, S., Palmada, M., Bohmer, C., Vallon, V., 2003. Regulation of channels by the serum and glucocorticoid-inducible kinase – implications for transport, excitability and cell proliferation. *Cell. Physiol. Biochem.* 13, 41–50.
- Mahapatra, S., Marcantoni, A., Zuccotti, A., Carabelli, V., Carbone, E., 2012. Equal sensitivity of Cav1.2 and Cav1.3 channels to the opposing modulations of PKA and PKG in mouse chromaffin cells. *J. Physiol.* 590, 5053–5073.
- Marcantoni, A., Vandael, D.H., Mahapatra, S., Carabelli, V., Sinnegger-Brauns, M.J., Striessnig, J., Carbone, E., 2010. Loss of Cav1.3 channels reveals the critical role of L-type and BK channel coupling in pacemaking mouse adrenal chromaffin cells. *J. Neurosci.* 30, 491–504.
- Margheri, M., Pacini, N., Tani, A., Nosi, D., Squecco, R., Dama, A., Masala, E., Francini, F., Zecchi-Orlandini, S., Formigli, L., 2012. Combined effects of melatonin and all-trans retinoic acid and somatostatin on breast cancer cell proliferation and death: molecular basis for the anticancer effect of these molecules. *Eur. J. Pharmacol.* 681, 34–43.
- Naziroğlu, M., Tokat, S., Demirci, S., 2012. Role of melatonin on electromagnetic radiation-induced oxidative stress and Ca^{2+} signaling molecular pathways in breast cancer. *J. Recept. Signal Transduct. Res.* 32, 290–297.
- Novara, M., Baldelli, P., Cavallari, D., Carabelli, V., Giaccipoli, A., Carbone, E., 2004. Exposure to cAMP and β -adrenergic stimulation recruits Cav3 T-type channels in rat chromaffin cells through Epac cAMP-receptor proteins. *J. Physiol.* 558, 433–449.
- O’Grady, S.M., Lee, S.Y., 2005. Molecular diversity and function of voltage-gated (Kv) potassium channels in epithelial cells. *Int. J. Biochem. Cell Biol.* 37, 1578–1594.
- Ohkubo, T., Yamazaki, J., 2012. T-type voltage-activated calcium channel Cav3.1, but not Cav3.2, is involved in the inhibition of proliferation and apoptosis in MCF-7 human breast cancer cells. *Int. J. Oncol.* 41, 267–275.
- Ouadid-Ahidouch, H., Ahidouch, A., 2008. K^+ channel expression in human breast cancer cells: involvement in cell cycle regulation and carcinogenesis. *J. Membr. Biol.* 221, 1–6.
- Pardo, L.A., 2004. Voltage-gated potassium channels in cell proliferation. *J. Physiol.* 19, 285–292.
- Prakriya, M., Lingle, C.J., 1999. BK channel activation by brief depolarizations requires Ca^{2+} influx through L- and Q-type Ca^{2+} channels in rat chromaffin cells. *J. Neurophysiol.* 81, 2267–2278.
- Rich, A., Farrugia, G., Rae, J.L., 1999. Effects of melatonin on ionic currents in cultured ocular tissues. *Am. J. Physiol.* 276, C923–C929.
- Sánchez-Barceló, E.J., Mediavilla, M.D., Alonso-Gonzalez, C., Rueda, N., 2012. Breast cancer therapy based on melatonin. *Recent Pat. Endocr. Metab. Immune Drug Discov.* 6, 108–116.
- Sbrana, F., Sassoli, C., Nosi, D., Squecco, R., Paternostro, F., Tiribilli, B., Zecchi-Orlandini, S., Francini, F., Formigli, L., 2008. Role for stress fiber contraction in surface tension development and stretch-activated channel regulation in C2C12 myoblasts. *Am. J. Physiol. Cell Physiol.* 295, 160–172.
- Srinivasan, V., Spence, D.W., Pandi-Perumal, S.R., Trakht, I., Cardinali, D.P., 2008. Therapeutic actions of melatonin in cancer: possible mechanisms. *Integr. Cancer Ther.* 7, 189–203.
- Sundelacruz, S., Levin, M., Kaplan, D.L., 2009. Role of membrane potential in the regulation of cell proliferation and differentiation. *Stem Cell Rev.* 5, 231–246.
- Vijayalaxmi, T.C.R., Reiter, R.J., Herman, T.S., 2002. Melatonin: from basic research to cancer treatment clinics. *J. Clin. Oncol.* 20, 2575–2601.
- Wang, Z., 2004. Roles of $K(+)$ channels in regulating tumour cell proliferation and apoptosis. *Pflug. Arch.* 448, 274–286.
- Wang, X.T., Nagaba, Y., Cross, H.S., Wrba, F., Zhang, L., Guggino, S.E., 2000. The mRNA of L-type calcium channel elevated in colon cancer: protein distribution in normal and cancerous colon. *Am. J. Pathol.* 157, 1549–1562.